DOI: 10.1002/chem.200500383

Expanding the Number of Stable Isomeric Structures of the C_{80} Cage: A New Fullerene $Dy_3N@C_{80}$

Shangfeng Yang* and Lothar Dunsch*[a]

Abstract: The production, isolation, and spectroscopic characterization of a new $Dy_3N@C_{80}$ cluster fullerene that exhibits three isomers (**1**–**3**) is reported for the first time. In addition, the third isomer (**3**) forms a completely new C_{80} cage structure that has not been reported in any endohedral fullerenes so far. The isomeric structures of the $Dy_3N@C_{80}$ cluster fullerene were analyzed by studying HPLC retention behavior, laser desorption time-of-flight (LD-TOF) mass spectrometry, and UV-Vis-NIR and FTIR spectroscopy. The three isomers of $Dy_3N@C_{80}$ were all large band-gap (1.51, 1.33, and 1.31 eV for **1**–**3**, respectively) materials, and could be classified as very stable fullerenes. According to results of FTIR spectroscopy, the $Dy_3N@C_{80}$ (I) (**1**) was assigned to the fullerene cage C_{80}:7 (I_h), whereas $Dy_3N@C_{80}$ (II) (**2**) had the cage structure of C_{80}:6 (D_{5h}). The most probable cage structure of $Dy_3N@C_{80}$ (III) (**3**) was proposed to be C_{80}:1 (D_{5d}). The significant differences between $Dy_3N@C_{80}$ and other reported $M_3N@C_{80}$ (M = Sc, Y, Gd, Tb, Ho, Er, Tm) cluster fullerenes are discussed in detail, and the strong influence of the metal on the nitride cluster fullerene formation is concluded.

Keywords: chromatography · endohedral fullerenes · isomers · nitrides · spectroscopy

Introduction

Endohedral fullerenes exhibit a variety of novel properties, such as peculiar redox and photoelectrochemical behavior, luminescence, paramagnetism, and enhanced nonlinear optical response.[1–6] Specifically, trimetallic nitride endohedral fullerenes (cluster fullerenes), a new class of fullerenes with an encaged trimetallic nitride cluster, have attracted great interest since their discovery by Dorn et al. in 1999.[7] This is due to, not only the feasibility of tuning the trapped metal atoms and of stabilizing a large variety of cage sizes, including different isomeric structures, but also to the demonstration of several distinguishing properties[4,7–10] that indicate potential applications, such as their use as new contrast agents in magnetic resonance imaging (MRI).[4,5,11]

$Sc_3N@C_{80}$, the most abundant member of the trimetallic nitride cluster fullerenes, can be formally viewed as a positively charged, planar cluster inside a negatively charged C_{80} cage.[7,12] Regardless of the successful production of trimetallic nitride cluster fullerenes based on, not only Sc_3N encaged in other cages, such as C_{78}[13] and the non-IPR (isolated pentagon rule) C_{68} cage,[14] but also other M_3N (M = Y,[10] Gd,[15] Tb,[16] Ho,[9] Er,[4,7,17] Tm,[18] Lu[19,20]) cluster fullerenes, the C_{80}:7 (I_h) cage isomer[21] was recognized as the most abundant fullerene cage.[4] Among these new cluster fullerenes, Tm_3N and Gd_3N, which were produced recently by our group, appear quite peculiar, due to their unusually large cage-size distributions.[15,18] In addition to the observation that Gd_3N is the largest cluster encaged in fullerene cages to date,[15] another remarkable uniqueness of the $Gd_3N@C_{80}$ cluster fullerene revealed recently is that Gd_3N nitride within the I_h C_{80} cage is pyramidal.[22] On the basis of a systematic comparison with reported lanthanide-based cluster fullerenes, a strong influence of the metal-ion radius (r) on the size of the encaged nitride cluster, and consequently, on the nitride cluster fullerene formation in terms of at least production yield and cage-size distribution, was revealed. For instance, $Gd_3N@C_{2n}$ cluster fullerenes exhibit, not only much lower yields, but also smaller cage-size distribution ($40 \le n \le 44$) than $Tm_3N@C_{2n}$ ($38 \le n \le 44$), primarily because the r of Gd^{3+} (0.94 Å) is larger than that of Tm^{3+} (0.87 Å).[15,18,23] Likewise, other M_3N (M = Tb, Ho, Er; r = 0.92, 0.90, and 0.88 Å,[23] respectively) cluster fullerenes show smaller cage-size distributions than the Tm_3N cluster

[a] Dr. S. Yang, Prof. Dr. L. Dunsch
Group of Electrochemistry and Conducting Polymers
Leibniz-Institute for Solid State and Materials Research Dresden
01171 Dresden (Germany)
Fax: (+49) 351-4659-745 (Dr. Yang)
Fax: (+49) 351-4659-811 (Prof. Dr. Dunsch)
E-mail: s.yang@ifw-dresden.de
l.dunsch@ifw-dresden.de

fullerene,[4,18] whereas the production of La_3N cluster fullerenes failed, presumably due to the large r of La^{3+} (1.06 Å).[9,23] Therefore, a plausible rule may be that the larger metal-ion radius r (cluster size) results in lower yield and smaller cage-size distribution for the cluster fullerenes, although this has yet to be confirmed. Specifically, dysprosium (Dy^{3+}) has a relatively large r (0.91 Å),[23] which is comparable to that of Tb^{3+} and Ho^{3+}, but much larger than that of Tm^{3+}. It would, therefore, be important to investigate whether the Dy_3N cluster fullerenes could be produced, and whether they would exhibit lower yields and smaller cage-size distributions, following the rule proposed above, than the Tm_3N cluster fullerenes.

On the other hand, the coexistence of the second isomer of $M_3N@C_{80}$ (M = Sc, Tm, Gd), showing quite different cage structure (C_{80}:6 (D_{5h})) and electronic properties to the first isomer, has been also demonstrated.[15,18,24,25] Therefore, a question worth addressing is whether the coexistence of two cage isomers provides another general rule for the other $M_3N@C_{80}$ cluster fullerenes. Moreover, because the results of theoretical studies indicate that there are seven isomers of the C_{80} cage that obey the IPR,[21] another intriguing question is: Does another stable isomeric form of this cage exist?

Here, we report on the production, isolation, and spectroscopic characterization of a novel $Dy_3N@C_{80}$ cluster fullerene, as well as a C_{80} cage structure of the third isomer that has never before been reported as a stable endohedral fullerene structure. HPLC and laser desorption time-of-flight (LD-TOF) mass spectrometry were used to isolate and identify the isomeric structures of the $Dy_3N@C_{80}$ cluster fullerene. Electronic properties and band-gaps of the three isomers were investigated by UV-Vis-NIR spectroscopy. The vibrational structures of the isomers were examined by using FTIR spectroscopy and compared with the other reported $M_3N@C_{80}$ (M = Sc, Tm, Gd) cluster fullerenes to determine their cage symmetries.

Results and Discussion

Isolation and identification of the three isomers of the $Dy_3N@C_{80}$ cluster fullerene (1–3): A typical chromatogram of a fullerene extract mixture is shown in Figure 1a (curve A), indicating the formation of $Dy_3N@C_{2n}$ cluster fullerenes, which will be discussed below. The chromatogram shows that **1** and **2** are the main products and **3** is produced in a much lower yield. These three products can be assigned to $Dy_3N@C_{80}$, based on the results of mass spectroscopic (MS) analysis (Figure 2). Because **1**–**3** have quite different retention times, but the same molecular formula, it is concluded that they are different isomeric forms of $Dy_3N@C_{80}$, denoted as $Dy_3N@C_{80}$ (I), $Dy_3N@C_{80}$ (II), and $Dy_3N@C_{80}$ (III), respectively (see Table 1). At this stage, despite the existence of the completely novel third isomer **3**, it can be confirmed that the two main isomers of the C_{80} cage also exist for $Dy_3N@C_{80}$ and, hence, such a coexistence is proven as a general rule for the $M_3N@C_{80}$ cluster fullerene.[15,18,24,25]

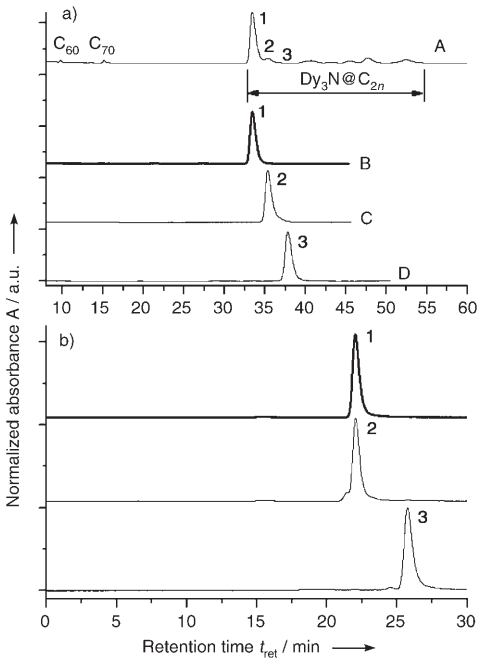

Figure 1. a) Chromatograms of a $Dy_3N@C_{2n}$ fullerene extract mixture (A) and the isolated isomers of $Dy_3N@C_{80}$, **1** (B), **2** (C), and **3** (D) (linear combination of two 4.6×250 mm Buckyprep columns; flow rate 1.6 mL min^{-1}; injection volume 100 µl; toluene as eluent (mobile phase); 40 °C). The peaks with t_{ret} = 32.7 ~ 54.7 min correspond to $Dy_3N@C_{2n}$ ($39 \le n \le 44$) cluster fullerenes. b) Chromatograms of the three isolated isomers of $Dy_3N@C_{80}$ **1**–**3**, which were run on a Buckyclutcher column (flow rate 1.0 mL min^{-1}; injection volume 100 µL; toluene as eluent; 20 °C).

In the fullerene extract, the most abundant product is **1** (t_{ret} = 33.4 min, Figure 1a). This agrees well with previous studies of $M_3N@C_{2n}$ (M = Sc, Tm) cluster fullerenes, which revealed the unusually high yield for $M_3N@C_{80}$.[18,24] Excluding **2** and **3**, the abundance of **1** is approximately 25-times

Table 1. Characteristics of the three isolated isomers of the $Dy_3N@C_{80}$ cluster fullerene (**1**–**3**).

Product	Isomer	Retention time t_{ret} [min]		Purity[a]	Onset	Band-gap[b]	UV-Vis-NIR	Color[c]
		Buckyprep	Buckyclutcher	[%]	[nm]	[eV]	absorption peaks [nm]	
1	$Dy_3N@C_{80}$ (I)	33.4	22.0	≥99	823	1.51	320, 401, 554, 626, 643, 670, 700	orange
2	$Dy_3N@C_{80}$ (II)	35.3	22.0	≥98	929	1.33	463, 627, 714	dark yellow
3	$Dy_3N@C_{80}$ (III)	38.2	25.7	≥95	948	1.31	429, 557, 673, 735	yellow

[a] Based on integration results of chromatograms recorded from runs on both Buckyprep and Buckyclutcher columns, and LD-TOF mass spectra obtained in positive-ion mode. [b] The band-gap is calculated from the onset (band-gap (eV) ≈ 1240/onset (nm)). [c] When dissolved in toluene.

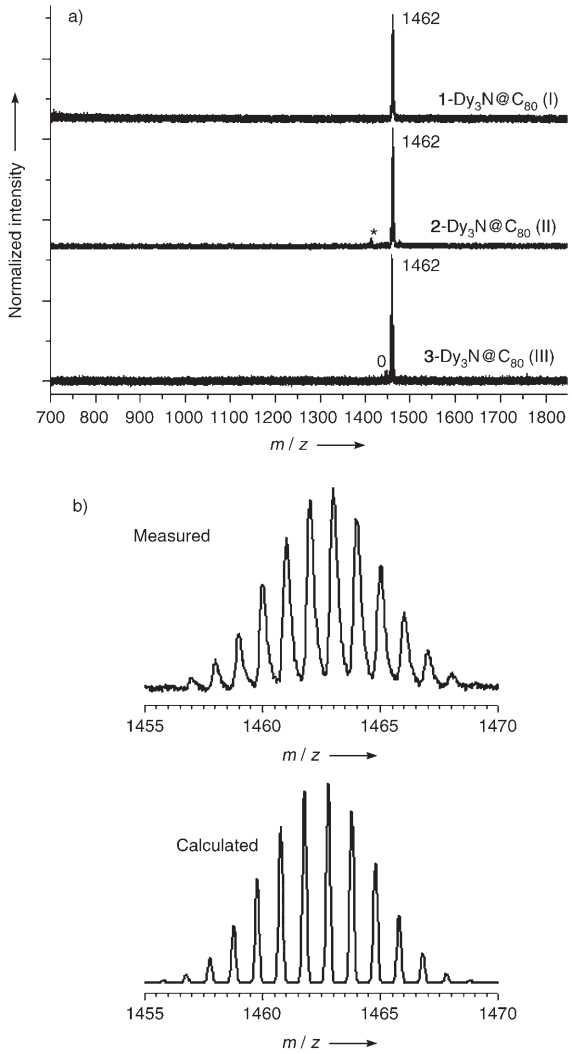

Figure 2. a) Positive-ion LD-TOF mass spectrum of the three isolated isomers of $Dy_3N@C_{80}$ **1–3**. The asterisk and open circle represent the nonseparable minor impurities of $Dy_3N@C_{76}$ and $Dy_3@C_{80}$, respectively. b) The measured and calculated isotope distributions of $Dy_3N@C_{80}$ **1–3**. The measured isotope distribution is based on the peaks at m/z 1462 shown in (a), and is the same for **1–3**.

that of C_{60} ($t_{ret}=9.6$ min), as estimated from the HPLC peak intensity. This relative yield of **1** to C_{60} is much higher than that of the other $M_3N@C_{80}$ (M = Sc, Y, Gd, Tb, Ho, Er, Tm) cluster fullerenes reported to date.[4,7–10,13–20,22,24,25] On the other hand, the abundance of **1** is 65–70% that of all other fullerenes. This is similar to other $M_3N@C_{80}$ (M = Sc, Y, Tb, Ho, Er, Tm) cluster fullerenes,[4,18,24] but much higher than that of $Gd_3N@C_{80}$.[15,22]

For the second isomer **2** ($t_{ret}=35.3$ min, shoulder peak in Figure 1a), its relative abundance is approximately 10% of the entire $Dy_3N@C_{80}$ fraction, comparable to that for $Gd_3N@C_{80}$ (II), but only half as high as for $Sc_3N@C_{80}$ (II) and $Tm_3N@C_{80}$ (II).[15,18,24] However, the third isomer **3** ($t_{ret}=38.2$ min) has a relative abundance of three orders of magnitude lower than **1**, but is still separable. Such a low yield of **3** suggests that it has a much lower stability and/or lower formation selectivity than the other two isomers. As **3** has a band-gap comparable to that of **2** (Table 1), which may generally indicate the stability of fullerene, the lower formation selectivity of **3** is responsible for its lower yield. Comparison of the $Dy_3N@C_{80}$ cluster fullerenes with the other $M_3N@C_{80}$ (M = Sc, Tm, Gd) cluster fullerenes that we reported previously[15,18,24] revealed that the retention times of the two isomers of $Dy_3N@C_{80}$ (**1**, **2**) were slightly smaller. This was because the experimental conditions adopted for the two different HPLC techniques used gave differences in isolation performance.

Chemical identities and purities of the isolated isomers of $Dy_3N@C_{80}$ (**1–3**) were ascertained from chromatograms of runs performed on both Buckyprep (curves B–D in Figure 1a) and Buckyclutcher (Figure 1b) columns, together with results of LD-TOF MS analysis, as shown in Figure 2a. The considerably high purity of all three isomers could then be concluded (Table 1), although **2** and **3** contain small amounts of other nonseparable fullerenes. A closer comparison of the measured isotope distributions for the $Dy_3N@C_{80}$ isomers with the theoretical calculations indicates fairly good agreement, as demonstrated in Figure 2b, confirming the proposed chemical signatures. Moreover, **1** and **2** have equal t_{ret} on a Buckyclutcher column, but the t_{ret} of **3** on both Buckyprep and Buckyclutcher columns are much larger than that of **1** and **2**. This suggests differences in their dipole and/or quadrupole moments,[26] which are caused by the different charge distributions dependent on the cage symmetry, as will be discussed below.

Comparison of the $Dy_3N@C_{2n}$ cluster fullerenes with other $M_3N@C_{2n}$ (M=Sc, Y, Gd, Tb, Ho, Er, Tm, Lu) cluster fullerene families: Further MS analysis of the fullerene extract indicates the formation of $Dy_3N@C_{2n}$ cluster fullerenes with cages ranging from C_{76} ($n=38$) to C_{98} ($n=49$). This $Dy_3N@C_{2n}$ ($38\leq n\leq 49$) family is much larger than all of the other $M_3N@C_{2n}$ (M = Sc, Y, Gd, Tb, Ho, Er, Tm, Lu) cluster fullerene families reported to date.[4,7–10,13,20,24,25] The systematic isolation and detailed characterization of the whole family, focussing on the dominant fractions with t_{ret} of 32.7~54.7 min ($Dy_3N@C_{2n}$, $39\leq n\leq 44$), will be reported elsewhere.[27]

Indeed, the formation of $Dy_3N@C_{2n}$ cluster fullerenes with cages smaller than C_{80}, such as C_{76} and C_{78}, which are absent in the $Gd_3N@C_{2n}$ family, reveals another remarkable difference between $Dy_3N@C_{2n}$ and $Gd_3N@C_{2n}$ cluster fullerenes.[27] The cluster size constraint resulting from the large Gd_3N nitride vanishes completely for the Dy_3N nitride cluster.[15] By using the common method to estimate the diameter of the M_3N cluster ($d(M_3N)\propto 4r(M^{3+})$),[15,23] it is found that the Dy_3N cluster is only ~0.12 Å smaller than the Gd_3N cluster, but much larger than the Sc_3N and Tm_3N clusters. In the periodic table, Dy is located between Gd and Tm for the lanthanide elements, according to atomic number. It appears that the $Dy_3N@C_{80}$ cluster fullerene resembles $Tm_3N@C_{80}$ more closely than $Gd_3N@C_{80}$, as described below.

In general, all of these distinct differences reveal the uniqueness of the $Dy_3N@C_{80}$ cluster fullerene. The plausible rule proposed earlier—the larger metal-ion radius *r* (cluster size) results in lower yield and smaller cage-size distribution—unambiguously fails for the present case of $Dy_3N@C_{2n}$ cluster fullerenes. Because the same type and strength of cluster-cage interaction has been concluded for the different $M_3N@C_{80}$ (M = Sc, Y, Gd, Tb, Ho, Er, Tm) cluster fullerenes, and this is assumed to be also applicable for $Dy_3N@C_{80}$,[15] it is expected that the cluster-cage interaction plays a less important role in the relative yields of these cluster fullerenes than in cluster size (metal-ion radius *r*) and metal–nitrogen bond strength.

Electronic absorption spectra of the three isolated isomers of the $Dy_3N@C_{80}$ cluster fullerene (1–3): The UV-Vis-NIR spectra of the three isolated isomers of $Dy_3N@C_{80}$ **1–3** dissolved in toluene show characteristic electronic absorptions (Figure 3 and Table 1). Firstly, the optical band-gap could be

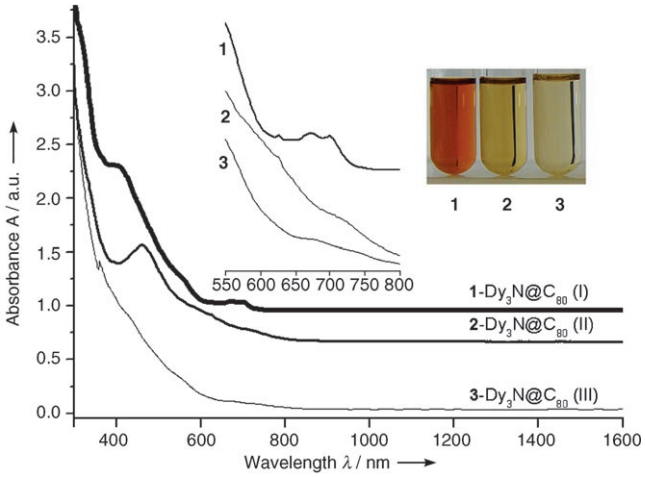

Figure 3. UV-Vis-NIR spectra of the three isolated isomers of $Dy_3N@C_{80}$ **1–3** dissolved in toluene. The insets show the enlarged spectral range (550–800 nm) and the photographs of **1–3** dissolved in toluene.

estimated according to the onset of the electronic absorption spectrum.[1,4,7,15,18,24] Based on the spectral onsets of 823, 929, and 948 nm for **1**, **2**, and **3**, respectively, the band-gaps of **1–3** are calculated to be 1.51, 1.33, and 1.31 eV, respectively. Assuming the borderline of 1.0 eV to distinguish large and small band-gap fullerenes,[18,24] we may conclude that the three isomers of the $Dy_3N@C_{80}$ cluster fullerene, similar to the other known $M_3N@C_{80}$ (M = Sc, Y, Gd, Tb, Ho, Er, Tm) cluster fullerenes,[4,15,18,24] are all large band-gap materials and electronically stable fullerenes.

Electronic absorptions are due predominantly to π–π^* transitions of the fullerene cage and depend on the structure and charge state of the cage.[1,4] The HOMO–LUMO transition of **1** has a doublet structure with absorption maxima at 700 and 670 nm (see inset of Figure 3), and the strongest visible absorption peak at 401 nm, along with a shoulder peak at 554 nm. All of these features are quite similar to those of the other $M_3N@C_{80}$ (I) (M = Sc, Tb, Ho, Y, Er, Tm, Gd) counterparts,[4,15,18,24] indicating their identities in the cage symmetries and electronic structures. Likewise, by comparing the UV-Vis-NIR spectrum of **2** with the other corresponding $M_3N@C_{80}$ (II) (M = Sc, Tm) cluster fullerenes,[18,24] we see a fairly close resemblance. For instance, **2** exhibits the HOMO–LUMO transition at 714 nm (710 nm for $Tm_3N@C_{80}$ (II)) and the strongest visible absorption peak at 463 nm (460 and 426 nm for $Tm_3N@C_{80}$ (II) and $Sc_3N@C_{80}$ (II), respectively), along with a shoulder peak at 627 nm (625 nm for $Tm_3N@C_{80}$ (II)).[18,24] On the other hand, **3** exhibits less distinct features than the other two isomers, showing only very weak absorption maxima at 735 and 673 nm, along with two shoulder peaks at 557 and 429 nm. For comparison, there are apparent differences between the UV-Vis-NIR spectra of **1–3** and that of $Dy_2@C_{80}$ (I), which exhibits weak absorptions at 600 and 688 nm, together with the NIR absorption at 1133 nm.[28] This rules out similarities in their electronic structure.

Based on these different absorption properties, the three isomers of $Dy_3N@C_{80}$ **1–3** show quite distinct colors, as clearly illustrated in the inset of Figure 3. In fact, like **1**, the other $M_3N@C_{80}$ (I) (M = Sc, Tb, Ho, Y, Er, Tm, Gd) cluster fullerenes also have an orange color, due to their specific absorption bands in the visible region.[4,15,18,24] The color of **2** (dark yellow) is same as that of $Tm_3N@C_{80}$ (II), but slightly different to $Sc_3N@C_{80}$ (II) (light brown).[18,24] Isomer **3** is yellow after dissolving in toluene, much lighter than the other two isomers.

Cage structure assignment of the three isomers of the $Dy_3N@C_{80}$ cluster fullerene (1–3) by FT-IR spectroscopy: As we demonstrated before, infrared spectroscopy is a powerful tool for the structural analysis of fullerenes, not only due to its high structural sensitivity, but also because of its higher time resolution compared to NMR spectroscopy.[4,8,10,15,18,24] Figure 4 shows the FTIR spectra of **1** (curve a) and **2** (curve e), along with their counterparts $M_3N@C_{80}$ (I) (M = Sc, Tm, Gd) (curves b–d) and $M_3N@C_{80}$ (II) (M = Sc, Tm) (curves f and g) for comparison. The FTIR spectrum of **1** shows fewer lines, which are almost identical to those of the other known $M_3N@C_{80}$ (I) (M = Sc, Tb, Ho, Y, Er, Tm, Gd) icosahedral structures.[4,8,15,18,24] A detailed analysis reveals five groups of tangential cage modes for all of the C_{80} (I) isomers, labeled as B, C, D, F, and H, according to reference [10], and one strong radial cage mode at around 500 cm^{-1}.[15,18,24] Due to these close similarities, **1** ($Dy_3N@C_{80}$ (I)) is assigned to the same fullerene cage as the other known $M_3N@C_{80}$ (I) (M = Sc, Tb, Ho, Y, Er, Tm, Gd) cluster fullerenes, that is, C_{80}:7 with I_h symmetry (see Figure 6b). Such an assignment is strongly supported by results of the HPLC and UV-Vis-NIR analysis, as described above.

The FTIR spectrum of **2** ($Dy_3N@C_{80}$ (II)) shows a similar resemblance to that of the known $M_3N@C_{80}$ (II) (M = Sc, Tm), in terms of all of the characteristic vibrational modes.

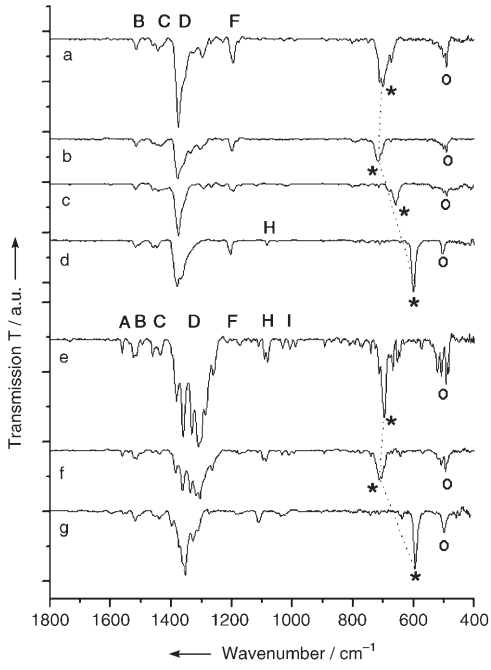

Figure 4. FTIR spectra of (a) $Dy_3N@C_{80}$ (I), (b) $Tm_3N@C_{80}$ (I), (c) $Gd_3N@C_{80}$ (I), (d) $Sc_3N@C_{80}$ (I), (e) $Dy_3N@C_{80}$ (II), (f) $Tm_3N@C_{80}$ (II), and (g) $Sc_3N@C_{80}$ (II) (500 accumulations, 2 cm^{-1} resolution). The capital letters refer to the line-group classification introduced in reference [10]. The asterisks and the open circles mark the antisymmetric M–N stretching vibrational modes and radial cage modes, respectively. The dotted lines indicate the metal-induced shifts of antisymmetric M–N stretching vibrational modes.

Therefore, the fullerene cage structure can be unambiguously identified as C_{80}:6 (D_{5h}) (see Figure 6c).[18,21,25] On the other hand, it is noted that the FTIR spectrum of **2** has signatures quite similar to those of **1**, although the line-group splitting for the former isomer is much stronger than for the latter one.

A closer examination of these FTIR spectra reveals a noteworthy difference in their most intense, low-energy IR lines, which can be assigned to the antisymmetric M–N stretching vibrations of the M_3N clusters, due to the comparable intensity and strong metal dependences.[4,15,18,24] For $Dy_3N@C_{80}$ (I) (**1**), the strongest low-energy IR line is at around 702 cm^{-1}, which is almost the same as for $Tm_3N@C_{80}$ (I) (710 cm^{-1}), but much higher than those of $Gd_3N@C_{80}$ (I) (657 cm^{-1}) and $Sc_3N@C_{80}$ (I) (599 cm^{-1}).[15,18,24] The antisymmetric M–N stretching vibrational mode of $M_3N@C_{80}$ (II) shows the same features. The lower vibrational energy reflects a weaker metal–nitrogen bond, which influences strongly the abundance of cluster fullerene formation.[15] It is, therefore, reasonable to deduce that $Dy_3N@C_{80}$ resembles $Tm_3N@C_{80}$ more closely than $Gd_3N@C_{80}$ or $Sc_3N@C_{80}$, based on the identical antisymmetric M–N stretching vibrations of the former two, and the dramatic metal-induced down-shifts of the vibrational frequencies of the latter two (see dotted lines in Figure 4). This conclusion coincides well with the relative abundancies of these $M_3N@C_{80}$ structures, as revealed by the chromatograms discussed above.

The FTIR spectrum of the novel third isomer **3** is, however, quite different from those of the other two isomers, as shown in Figure 5. Firstly, it can be seen that the antisymmetric Dy–N stretching vibrational mode (~702 cm^{-1}) of the Dy_3N cluster for **3** is the same as for **1** and **2**, although the intensity is the strongest of all of the cage modes. On the other hand, the tangential cage modes presented for **1** and **2** are also detected for **3**, regardless of the lower intensities, although the strong radial cage mode at around 500 cm^{-1} is surprisingly missing (see dashed arrow). Instead, several new vibrational lines between 750–1700 cm^{-1} with considerably high intensities appear beyond the usual region for the tangential cage modes. To confirm this spectrum, a repeated heat treatment in high vacuum ($<10^{-6}$ mbar) was conducted, resulting in an identical spectrum. Therefore, no impurities of solvents are responsible for these new lines. The origins of these unusual vibrational modes of the fullerene and the reason for the disappearance of the typical radial cage mode are not yet fully understood. These could be elucidated by group theory calculation and further analysis of the metal dependence, which should indicate whether such a C_{80} isomer might also exist for cluster fullerenes based on other metals. Nevertheless, the detailed analysis reveals that the total number of infrared active lines in the FTIR spectrum of **3** is actually comparable to that of **2**. Such a small

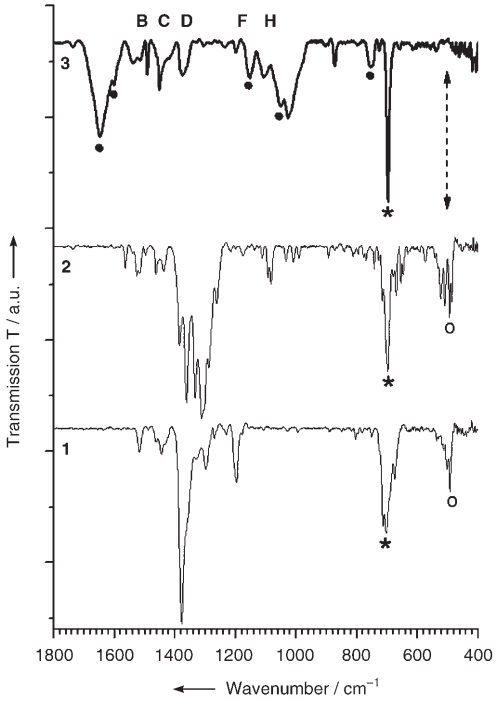

Figure 5. FTIR spectra of **3** (top trace) and **1**–**2** (lower traces, copied from Figure 4). The capital letters, asterisks, and open circles represent the same features as in Figure 4. The filled circles mark the new vibrational modes, which are absent in the spectra of **1** and **2**.

number of infrared active lines could be interpreted only as the three C_{80} cage isomers with highest symmetries, that is, C_{80}:1, C_{80}:6, and C_{80}:7, based on the selection rules.[18,21,24] As the other four cages give significantly more infrared active lines (from 116 to 178), they could then be excluded.[18,21,24] Given that C_{80}:7 and C_{80}:6 have already been assigned to the two main isomers **1** and **2**, C_{80}:1 (D_{5d})[21,29] appears to be the most probable cage structure for **3**. With this assignment, the ellipsoidal cage could account partly for the larger retention time of **3** than **1** and **2** on both Buckyprep and Buckyclutcher columns, as mentioned above. Based on these results, the cage structure of **3** is schematically demonstrated by the models shown in Figure 6, together with those of **1** and **2** for comparison, clearly indicating their significant differences in cage symmetries. To our knowledge, the D_{5d} isomer was experimentally isolated only for the empty C_{80} cage, which indicates the reasonably high stability,[29] and no endohedral fullerenes based on such a cage have been isolated and characterized until now.

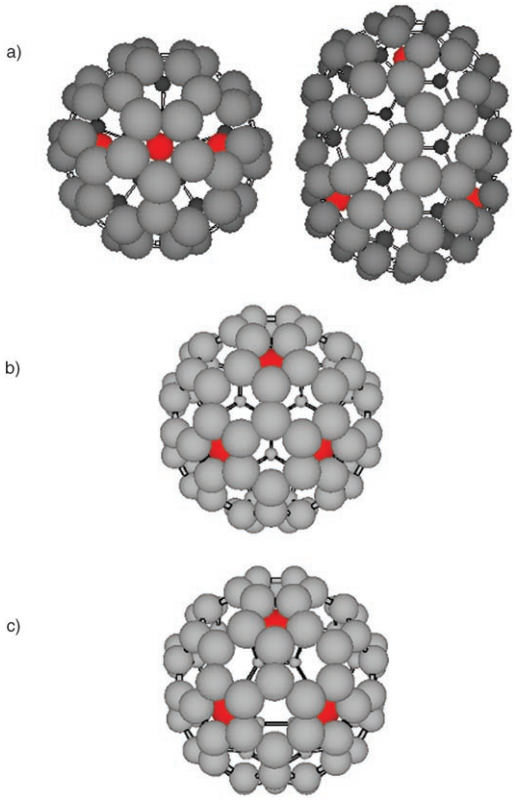

Figure 6. a) Schematic structure model of **3** (D_{5d}) in two views. left: top view along the main C_5 axis, assuming that one Dy atom locates on the C_5 axis; right: front view. Structure models of **1** (I_h) (b) and **2** (D_{5h}) (c) are shown for comparison. The Dy and C atoms are drawn in red and grey, respectively. The N atoms are hidden by the central C or Dy atoms.

Conclusion

For the first time, we have successfully produced three isomers of $Dy_3N@C_{80}$ (**1**–**3**) at a high selectivity compared to the empty fullerenes. The three isomers of $Dy_3N@C_{80}$ **1**–**3** were isolated in high purity and characterized by UV-Vis-NIR and FTIR spectroscopy. All three are large band-gap (1.51, 1.33, and 1.31 eV, respectively) materials and can be classified as very stable fullerenes. $Dy_3N@C_{80}$ (I) (**1**) is assigned to the fullerene cage C_{80}:7 (I_h), whereas $Dy_3N@C_{80}$ (II) (**2**) has the cage structure of C_{80}:6 (D_{5h}). The most probable cage structure of $Dy_3N@C_{80}$ (III) (**3**) is proposed to be C_{80}:1 (D_{5d}), although this is to be confirmed by ongoing spectroscopic and theoretical investigations. Based on the analysis of both the relative abundancies and vibrational structures, it is concluded that $Dy_3N@C_{80}$ bears a closer resemblance to $Tm_3N@C_{80}$ than to $Gd_3N@C_{80}$ and $Sc_3N@C_{80}$. Furthermore, the uniqueness of the $Dy_3N@C_{80}$ cluster fullerene and the strong influence of the metal on the nitride cluster fullerene formation are illustrated by the distinct differences between $Dy_3N@C_{80}$ and other reported $M_3N@C_{80}$ (M = Sc, Y, Gd, Tb, Ho, Er, Tm) cluster fullerenes. Moreover, because of the feasibility of producing $Dy_3N@C_{80}$ (I) (**1**) with the highest relative yield to C_{60} of all of the other reported $M_3N@C_{80}$, **1** is particularly promising in potential applications, such as new contrast agents in magnetic resonance imaging (MRI).

Experimental Section

General procedures for the production of cluster fullerenes by a modified Krätschmer–Huffman DC-arc discharging method have been described elsewhere.[4,8,15,18,24,27] Briefly, a mixture of Dy_2O_3 and graphite powders was pressed into the hole of a graphite rod electrode in a molar ratio of 1:15 (Dy:C). As the source of nitrogen, 20 mbar NH_3 was introduced into the reactor atmosphere of 200 mbar He. After DC-arc discharging, the soot was collected under ambient conditions and firstly, pre-extracted with acetone for several hours, followed by the further Soxhlet extraction by CS_2 for 20 h. Cluster fullerene separation was achieved by performing single-stage HPLC using a Hewlett–Packard instrument (series 1050), with toluene as the eluent (mobile phase) at the flow rate of 1.6 mL min^{-1}. A linear combination of two analytical 4.6×250 mm Buckyprep columns (Nacalai Tesque, Japan) was applied to separate the three $Dy_3N@C_{80}$ isomers. A UV detector set to 320 nm was used for fullerene detection.

The purity of the isolated products was further checked by performing HPLC using a 10×250 mm Buckyclutcher column (Regis, USA) applying a flow rate of 1.0 mL min^{-1}, followed by LD-TOF MS analysis in both positive- and negative-ion modes (Biflex III, Bruker, Germany).

UV-Vis-NIR spectra of the three isolated isomers of $Dy_3N@C_{80}$ **1**–**3** dissolved in toluene were recorded by using a UV-Vis-NIR 3101-PC spectrometer (Shimadzu, Japan) at 1 nm resolution, and a quartz cell of 1 mm path length. For FTIR measurements, the three $Dy_3N@C_{80}$ isomers were drop-coated onto KBr single crystal disks. The residual toluene was removed by heating the polycrystalline films in a vacuum of 2×10^{-6} mbar at 235 °C for 3 h. The FTIR spectra were recorded at room temperature by using an IFS 66v spectrometer (Bruker, Germany).

Acknowledgements

Dr. M. Krause is acknowledged for valuable discussions. We also thank Mrs. H. Zöller, Ms. K. Leger, Mr. F. Ziegs, and Ms. S. Döcke cordially for technical assistance in the fullerene production, HPLC isolation, and spectroscopic characterizations. S.Y. thanks the Alexander von Humboldt (AvH) Foundation for financial support.

[1] H. Shinohara, *Rep. Prog. Phys.* **2000**, *63*, 843–892.
[2] *Endofullerenes: A New Family of Carbon Clusters* (Eds.: T. Akasaka, S. Nagase), Kluwer Academic, Dordrecht, Boston, London, **2002**.
[3] S. H. Yang, *Trends Chem. Phys.* **2001**, *9*, 31–43.
[4] L. Dunsch, M. Krause, J. Noack, P. Georgi, *J. Phys. Chem. Solids* **2004**, *65*, 309–315.
[5] L. J. Wilson, D. W. Cagle, T. P. Thrash, S. J. Kennel, S. Mirzadeh, J. M. Alford, G. J. Ehrhardt, *Coord. Chem. Rev.* **1999**, *192*, 199–207.
[6] S. F. Yang, PhD thesis, Hong Kong University of Science & Technology (Hong Kong), **2003**. See also a) S. F. Yang, S. H. Yang, *J. Phys. Chem. B* **2001**, *105*, 9406–9412; b) S. F. Yang, L. Z. Fan, S. H. Yang, *J. Phys. Chem. B* **2003**, *107*, 8403–8411; c) S. F. Yang, L. Z. Fan, S. H. Yang, *J. Phys. Chem. B* **2004**, *108*, 4394–4404; d) S. F. Yang, L. Z. Fan, S. H. Yang, *Chem. Phys. Lett.* **2004**, *388*, 253–258.
[7] S. Stevenson, G. Rice, T. Glass, K. Harich, F. Cromer, M. R. Jordan, J. Craft, E. Hajdu, R. Bible, M. M. Olmstead, K. Maitra, A. J. Fisher, A. L. Balch, H. C. Dorn, *Nature* **1999**, *401*, 55–57.
[8] L. Dunsch, P. Georgi, F. Ziegs, H. Zöller, DE-10301722-A1.
[9] L. Dunsch, P. Georgi, M. Krause, C. R. Wang, *Synth. Met.* **2003**, *135*, 761–762.
[10] M. Krause, H. Kuzmany, P. Georgi, L. Dunsch, K. Vietze, G. Seifert, *J. Chem. Phys.* **2001**, *115*, 6596–6605.
[11] E. B. Iezzi, F. Cromer, P. Stevenson, H. C. Dorn, *Synth. Met.* **2002**, *128*, 289–291.
[12] L. Alvarez, T. Pichler, P. Georgi, T. Schwieger, H. Peisert, L. Dunsch, Z. Hu, M. Knupfer, J. Fink, P. Bressler, M. Mast, M. S. Golden, *Phys. Rev. B* **2002**, *66*, 035107, 1–7.
[13] M. M. Olmstead, A. Bettencourt-Dias, J. C. Duchamp, S. Stevenson, D. Marciu, H. C. Dorn, A. L. Balch, *Angew. Chem.* **2001**, *113*, 1263–1265; *Angew. Chem. Int. Ed.* **2001**, *40*, 1223–1225.
[14] S. Stevenson, P. W. Fowler, T. Heine, J. C. Duchamp, G. Rice, T. Glass, K. Harich, E. Hajdu, R. Bible, H. C. Dorn, *Nature* **2000**, *408*, 427–428.
[15] M. Krause, L. Dunsch, *Angew. Chem.* **2005**, *117*, 1581–1584; *Angew. Chem. Int. Ed.* **2005**, *44*, 1557–1560.
[16] L. Feng, J. X. Xu, Z. J. Shi, X. R. He, Z. N. Gu, *Chem. J. Chin. Univ.* **2002**, *23*, 996–998.
[17] M. M. Olmstead, A. de Bettencourt-Dias, J. C. Duchamp, S. Stevenson, H. C. Dorn, A. L. Balch, *J. Am. Chem. Soc.* **2000**, *122*, 12220–12226.
[18] M. Krause, J. Wong, L. Dunsch, *Chem. Eur. J.* **2005**, *11*, 706–711.
[19] S. Stevenson, H. M. Lee, M. M. Olmstead, C. Kozikowski, P. Stevenson, A. L. Balch, *Chem. Eur. J.* **2002**, *8*, 4528–4535.
[20] E. B. Iezzi, J. C. Duchamp, K. R. Fletcher, T. E. Glass, H. C. Dorn, *Nano Lett.* **2002**, *2*, 1187–1190.
[21] P. W. Fowler, D. E. Manolopoulos, *An Atlas of Fullerenes*, Clarendon Press, Oxford, **1995**.
[22] S. Stevensen, J. P. Phillips, J. E. Reid, M. M. Olmstead, S. P. Rath, A. L. Balch, *Chem. Commun.* **2004**, 2814–2815.
[23] N. N. Greenwood, A. Earnshaw, *Chemistry of the Elements*, Pergamon Press, Oxford, **1984**.
[24] M. Krause, L. Dunsch, *ChemPhysChem* **2004**, *5*, 1445–1449.
[25] J. C. Duchamp, A. Demortier, K. R. Fletcher, D. Dorn, E. B. Iezzi, T. Glass, H. C. Dorn, *Chem. Phys. Lett.* **2003**, *375*, 655–659.
[26] D. Fuchs, H. Rietschel, R. H. Michel, A. Fischer, P. Weis, M. M. Kappes, *J. Phys. Chem.* **1996**, *100*, 725–729.
[27] S. F. Yang, L. Dunsch, *J. Phys. Chem. B*, **2005**, *109*, 12320–12328.
[28] N. Tagmatarchis, H. Shinohara, *Chem. Mater.* **2000**, *12*, 3222–3226.
[29] C.-R. Wang, T. Sugai, T. Kai, T. Tomiyama, H. Shinohara, *Chem. Commun.* **2000**, 557–558.

Received: April 5, 2005
Revised: June 10, 2005
Published online: October 13, 2005

